Characterization of responder profiles for cardiac resynchronization therapy through unsupervised clustering of clinical and strain data

Alban Gallard, Auriane Bidaut, Arnaud Hubert, Elif Sade, Sylvestre Marechaux, Marta Sitges, Jadranka Separovic-Hanzevacki, Virginie Le Rolle, Elena Galli, Alfredo Hernandez, et al.

Characterization of responder profiles for cardiac resynchronization therapy through unsupervised clustering of clinical and strain data

Running title: Strain clustering for cardiac resynchronization

Alban GALLARD[1,*], Auriane BIDAUT[1,*], Arnaud HUBERT[1], Elif SADE[2], Sylvestre MARECHAUX[3], Marta Sitges[4], Jadranka SEPAROVIC-HANZEVACKI[5], Virginie LE ROLLE[1], Elena GALLI[1], Alfredo HERNANDEZ[1,*], Erwan DONAL[1,*]

*: contribution of the two authors is identical

[1]: Univ Rennes, CHU Rennes, Inserm, LTSI - UMR 1099, F-35000 Rennes, France

[2]: Baskent University, Department of Cardiology Ankara, Turkey

[3]: Université Lille Nord de France, GCS-Groupement des Hôpitaux de l'Institut Catholique de Lille, Laboratoire d'échocardiographie, service de cardiologie, Centre des Valvulopathies, Faculté de Médecine et de Maïeutique, Université Catholique de Lille, France ; Laboratoire UPJCV, Université de Picardie, Amiens, France.

[4]: Cardiovascular Institute, Institut d'Investigacions Biomèdiques August Pi i Sunyer (IDIBAPS), Spain.

[5]: Department of Cardiovascular Diseases, University of Zagreb School of Medicine and UHC Zagreb, Zagreb 10000, Croatia

Correspondence

Erwan Donal, MD, PhD,

Service de Cardiologie - Hôpital Pontchaillou – CHU Rennes-

F-35033 RENNES

erwan.donal@chu-rennes.fr

Fax: +33299282510, Tel: +33299282525

Background: The mechanisms of improvement of left ventricular (LV) function with cardiac resynchronization therapy (CRT) are not yet elucidated. The aim of this study was to characterize CRT responder profiles through clustering analysis, based on clinical and echocardiographic pre-implantation data, integrating automatic quantification of longitudinal strain signals.

Methods: This is a multicenter observational study of 250 patients with chronic heart failure evaluated before CRT device implantation and followed up to four-years. Clinical, electrocardiographic and echocardiographic data were collected. Regional longitudinal strain signals were also analyzed with custom-made algorithms in addition to the existing approaches including the myocardial work indices. The response was defined as a decrease ≥15% in LV end-systolic volume. Death and hospitalization for heart failure at 4-years defined the adverse event rate. 70 features were analyzed using a clustering approach (k-means).

Results: 5 clusters were identified, with response rates between 50% in cluster 1 and 92.7% in cluster 5. These 5 clusters differed mainly by the characteristics of LV mechanics, evaluated by strain integrals. There was a significant difference in event-free survival at 4-year between cluster 1 and the other clusters. The quantitative analysis of strain curves, especially in the lateral wall was more discriminative than apical rocking, septal flash or myocardial work in most phenogroups.

Conclusions: Five clusters are described, defining groups of below-average to excellent responders. They demonstrate the complexity of LV mechanics and prediction of response to CRT. Automatic, quantitative analysis of longitudinal strain curves appears as a promising tool to improve the understanding of LV mechanics, patient characterization and selection for CRT.

Keywords: Cardiac resynchronization therapy; remodeling; echocardiography; strain imaging; machine learning; mechanical dyssynchrony

Word counts: 270 words

Introduction:

Current international guidelines recommend only clinical and electrocardiographic criteria to select patients for CRT, with no clear recommendations on the role of imaging for patient selection(1, 2). However, CRT corrects mechanical dyssynchrony through electrical stimulation(3, 4). Therefore, imaging techniques such as echocardiography have been studied and recent advances have been examined to understand different types of cardiac mechanical dyssynchronies and to consider them in relation to CRT(5, 6). Typically, in purely conduction disorders with a broad left bundle branch block (LBBB), there is an early activated septum that contracts prior to aortic valve opening and stretches the LV lateral wall(7). Contraction in the late activated lateral wall in this case causes a variable degree of systolic lengthening of the septum. This typical pattern of dyssynchrony could be influenced by the etiology of the cardiomyopathy, by loading conditions, diastolic or valvular characteristics. Therefore, there is not only one, but several kinds of mechanical dyssynchrony and this might explain why it has been so challenging to demonstrate the value of imaging techniques for selecting patients(8, 9). Also, CRT response is complex, with a great heterogeneity in patient characteristics.

An interesting approach to solve this complex evaluation of dyssynchrony is based on multiparametric analysis methods, and Machine Learning can be particularly useful in this context(10),[36]. The aim of this work is to evaluate a multiparametric clustering method integrating clinical and classical echocardiographic data, exploiting novel markers of the regional cardiac function, such as myocardial work and global longitudinal strain(5), to define

specific subgroups of CRT patients based on their baseline characteristics and their CRT response.

Material and Methods

Study population

We prospectively included patients from different centers in Europe who were eligible based on clinical grounds for CRT implantation according to the current European Society of Cardiology guidelines, and who consented to the study. These patients agreed to get their follow-up in the implanting center and they were not involved in a trial related to the device implanted. More specifically, these are chronic heart failure patients remaining symptomatic NYHA (New York Heart Association) II to III despite a step by step increase in the recommended medical treatments and management (all received beta-blockers, all received ACE-inhibitor or sacubitril-valsartan and all were on diuretics). Implantation was decided only after a careful follow-up and progressive optimization of medications. The patients were rather homogeneous in that careful pre-implantation optimization and implantations occurred between 2015 and 2019, (except 10 that were implanted before). Patients undergoing upgrades of pacemaker or implantable cardiac defibrillator were also included. Patients were evaluated systematically before CRT implantation and every 6-months after implantation.

Exclusion criteria were: non “I-A”, “I-B” indications for CRT according to ESC-guidelines (patients had LBBB and QRS > 130 ms but some had an atypical LBBB and QRS ≥150 ms), inadequate echocardiographic image quality according to the judgment of the investigator and absence of echocardiographic follow-up at 6 months(1). Patients in atrial fibrillation were also excluded.

The study was carried out in accordance with the principles outlined in the Declaration of Helsinki and was approved by the local ethical committee of each center.

Baseline and follow up evaluation

The baseline evaluation included clinical evaluation NYHA functional class, 6-min walking distance, laboratory testing, electrocardiographic (ECG) recording, echocardiographic evaluation of cardiac dimensions and function. These investigations were repeated at the 6 months follow up. Clinical information including cardiovascular risk factors, ECG and biological markers (creatinine, haemoglobin, sodium, NT-proBNP) was collected at baseline. The following aspects of the ECG were analyzed according to the guidelines: rhythm, PR interval duration, QRS axis, QRS duration and QRS morphology.

Echocardiography

Before implantation of the CRT device, patients were imaged by transthoracic echocardiography according to a predefined acquisition protocol (ViVid E9, S70 or E95, General Electric Healthcare, Horten, Norway). A complete echocardiogram including a speckle tracking analysis and global longitudinal strain (GLS) was performed and recorded for a core laboratory analysis (Inserm 1414 Clinical Investigation Center, Innovative Technology, Rennes, France 35000). Left atrial (LA) volume, right ventricular (RV) size and function were recorded according to recommendations (including RV strain free wall). Left ventricular ejection fraction (LVEF) and LV volumes were calculated using the biplane modified Simpson method. In order to obtain LV strain curves, two-dimensional grayscale images were acquired in the standard apical 4-chamber (4ch), 3-chamber (3ch), and 2-chamber (2ch) views, at a frame rate of at least 60 frames/s.

Mechanical dyssynchrony was quantified using a multi-parametric approach. Intra-ventricular dyssynchrony was defined by the visual presence of septal flash (SF) and/or apical rocking (AR)(11). SF is a premature and short contraction of the septum during the QRS and before the aortic valve opening. AR is a displacement of the LV-apex towards the lateral wall. (12) In addition to these two approaches, mitral inflow pattern and mitral inflow

duration were measured to determine atrioventricular dyssynchrony, defined as E/A duration < 40% of the cardiac cycle.

Offline echocardiographic analysis

Offline analysis was performed with a dedicated software (BT12-EchoPAC PC V202.0.0, GE Healthcare, Horten, Norway) to analyze all echocardiographic parameters, strain integrals, global longitudinal strain traces, and myocardial work on the pre-CRT implant echocardiogram. A line was traced along the endocardium's inner border in each of the three apical views on an end-systolic frame, and a region of interest was automatically defined between the endocardial and epicardial borders, with global longitudinal strain (GLS) then automatically calculated from the strain in the three apical views. For the 16 LV segments, the time to peak strain was determined and the standard deviation was calculated and named systolic mechanical dispersion, as previously proposed by Hasselberg et al.[12].

The calculated longitudinal strain signals for each segment were exported from the EchoPAC software. Each file was composed of longitudinal strain time series corresponding to 6 myocardial segments. These files were processed through a custom-made script in order to extract a set of features for further processing(5). These parameters are detailed in the paragraph "feature extraction" below. Myocardial work indices were calculated as previously reported(6, 13, 14).

Feature extraction

We analyzed 70 features (Appendix 1). 26 features were clinical and classical echocardiographic features, detailed in **Table 1**. These features were chosen among characteristics known to be correlated to CRT response(1, 11, 15). 44 features were automatically extracted from longitudinal strain curves of the apical 4ch view with a custom

Python program. Strain curves were obtained for 6 myocardial segments: basal-septal (BS), medio-septal (MS), apico-septal (AS), basal-lateral (BL), medio-lateral (ML), apico-lateral (AL). The features automatically extracted from strain traces have been already described and published by our team[5]. Briefly, these features are based on the estimation of the integral, or area over the curve, of each available strain signal, on different time supports. Hence, for each segment, different integrals are estimated. **Figure 1-B** shows an example of such extracted integral features for the Basal Lateral segment (BL) of a 4ch view. The first integral feature ($I_{avc}^{segment}$) is calculated from the beginning of the QRS to the instant of the aortic valve closure (**Figure 1-B, upper panel**). It represents a quantification of the cumulative strain developed by a given segment, which effectively contributes to LV ejection. A second integral ($I_{peak}^{segment}$) is calculated from the beginning of the QRS to the strain peak (**Figure 1-B, middle panel**). It represents the global cumulative strain developed by the contraction of the segment. The third integral is calculated as follows:

$$E^{segment} = I_{peak}^{segment} - I_{avc}^{segment}$$

and corresponds thus to the integral between the strain peak and the aortic valve closure (**Figure 1-B lower panel**). This is a marker of the mechanical efficiency of the segment. Positive values of this marker reflect an inefficient (or wasted) cumulative strain, acting after the closure of the aortic valve, when blood is no longer ejected.

This procedure was applied to all segments and to all views. Then, the mean of these different integrals was calculated for each view: I_{avc}^{Mean}, I_{peak}^{Mean} and E^{Mean}. The last set of features was based on the sums of integrals for the two walls Septal S and Lateral L (16): I_{avc}^{S}, I_{peak}^{S}, E^{S}, I_{avc}^{L}, I_{peak}^{L} and E^{L}.

These features represent the cumulative strain from all segments of a given wall. **Figure 1-C** shows, as an example, the two opposing walls of the 4ch view. Finally, the differences of the cumulative strain of the two sides were calculated as follows:

$$I_{avc}^{D} = I_{avc}^{L} - I_{avc}^{S}$$

$$I_{peak}^{D} = I_{peak}^{L} - I_{peak}^{S}$$

$$E^{D} = E^{L} - E^{S}$$

They are detailed below and shown in **Figure 1**. As in our previous works, strain integrals were calculated only for negative values under -5%:

- $T^{segment}$: time to peak strain for each segment (time to peak from QRS onset)
- T^{Mean}: average of all $T^{segment}$
- $P^{segment}$: amplitude of the peak of strain for each segment
- P^{Mean}: average of all $P^{segment}$
- $I_{avc}^{segment}$: integral between QRS onset and aortic valve closure for each segment (Integral of strain curve over time from QRS onset to the peak of strain)
- I_{avc}^{Mean}: average of all $I_{avc}^{segment}$
- $I_{peak}^{segment}$: integral between QRS onset and strain peak for each segment
- I_{peak}^{Mean}: average of all $I_{peak}^{segment}$
- $E^{segment}$: integral between the strain peak and the aortic valve closure.
- E^{Mean}: average of all $E^{segment}$
- I_{avc}^{S}: sum of $I_{avc}^{segment}$ septal segments
- I_{avc}^{L}: sum of $I_{avc}^{segment}$ lateral segments
- $I_{avc}^{D} = I_{avc}^{L} - I_{avc}^{S}$

- I^{S}_{peak}: sum of $I^{segment}_{peak}$ septal segments
- I^{L}_{peak}: sum of $I^{segment}_{peak}$ lateral segments
- $I^{D}_{peak} = I^{L}_{peak} - I^{S}_{peak}$
- E^{S}: sum of $E^{segment}$ septal segments
- E^{L}: sum of $E^{segment}$ lateral segments
- $E^{D} = E^{L} - E^{S}$

In a pre-processing phase, all features were normalized with the standard score before the application of the clustering algorithm. The original, non-normalized data were kept for the interpretation phase.

Clustering phase

K-means is a classical and widely-known clustering method [2,](17, 18)[,34,35]. The algorithm creates K different clusters. To do so, it finds a mean for each cluster which is the closest to each data point within the cluster (Appendix). We have chosen the K-means methods because of its low computational costs and because it produces tight clusters in comparison to other methods. One known disadvantage of this method is the sensitivity to the initial conditions. In our case, repetition on several runs using different initial conditions yielded no notable modification in the identified clusters. K-means and subsequent analyses were made using a custom script based on open-source library Sklearn under the Python language [37]. The choice of the optimal number of clusters K was determined using the Silhouette score, which is a measure of consistency within a cluster of data [32]. The Silhouette value is a measure of how similar an object is to its own cluster (cohesion) compared to other clusters (separation). The Silhouette score ranges from −1 to +1, where a higher value indicates that the object is well matched to its own cluster and poorly matched to neighboring clusters. In

order to determine the best number of clusters to generate, we calculated in this work the Silhouette score for the interval [2, 15] clusters.

Post-clustering feature-dimension reduction

Principal component analysis (PCA) transforms a large dataset into a dataset with fewer features named components. Since the obtained components are a combined marker of all initial features, they do not provide a direct physiological meaning. The obtained PCA components are ranked by the level of the variance of the original data that they capture [3].

In this work, PCA was applied after the clustering phase, mainly to provide a graphical representation of the clusters in a reduced space and to ease multi-variate characterization of each cluster. The three first principal components were used. Note that the clustering method was applied on the original, normalized features. In this manner, the separation of the individuals during the clustering method is performed on individual, interpretable features.

The correlation between each original feature and a given principal component can be readily obtained from the results of the PCA. These correlations can be plotted on each factorial plane (correlation plot), scaled, and superposed to the PCA feature project plot, in order to visualize how each feature contributes to each principal component and, therefore, to the constitution of each cluster. In this graph, the amplitude of the vectors (distance to the origin) represents the relative contribution of each feature to the factor map; features that are positively correlated are closely located and features that are negatively correlated present an opposite sign.

Rank test Analysis

A Wilcoxon signed-rank test was applied to establish how the clusters differ. For each feature, it was applied between a given cluster and the population composed of the

individuals of the four other clusters. This analysis indicates how a cluster is different from the others, in a feature-by-feature basis. For each cluster, we classified the features according to their rank test. The features with the best rank of a given cluster can be linked to the response rate of this cluster.

Response and adverse event rate

According to the prespecified protocol, at 12-month, the response was a reduction in left ventricular end-systolic volume (LVESV) of ≥ 15% (i.e. LV reverse remodeling) or an increase of 5% in LVEF. The patients respecting this criterion are named responders, otherwise they were considered non-responders.

The adverse event rate was a composite clinical criterion with occurrence of death, and/or hospitalization for heart failure. Kaplan-Meier estimates were used to construct the survival curves based on all available follow-up for the time-to-event analysis, for all obtained clusters. A log rank test was applied to compare each pair of clusters.

Results

254 patients were analyzed, and 250 patients were included in the final analysis. Four patients were not included in the analysis due to missing data. **Table 1** shows the patient characteristics. 185 responders were identified, representing 74% of the population.

According to the Silhouette score, the optimal number of clusters was identified as 5 clusters. Cluster 1 included 52 patients, 50 % of those being responders. Cluster 2 included 65 patients, with 70.8% responders. Cluster 3 was composed of 29 patients with a 72.4% responder rate. Cluster 4 contained 63 patients, with a rate of 85.7% of responders. Finally, cluster 5 included 41 patients with 92.7% responder rate.

As a confirmation, we also tested PCA with 15 principal components before clustering and we obtained the same clusters except for some patients that were borderline between 2

clusters. We chose to keep the clustering without previous PCA to offer more interpretability and to provide a comprehensive manuscript on the role of imaging in the field of CRT.

Figure 2 shows projected features for all patients in the space of the two first principal components of the PCA. The first principal component explains 23.4 % of the variance and 10.2 % for the second. So, the representation in the two principal component space explains 33.6 % of the variance. A plot of the second factorial axis, explaining 32.5% of the variance, was also analyzed but is not shown in the paper. Each patient is thus represented by a dot in this graph. Different colors represent the different obtained clusters. Responder patients are represented with a star sign. Note that, due to the projection of individuals on this plane, clusters do overlap. This does not occur in the 70-dimension space of the original features.

The arrows presented in **Figure 2** represent the variable correlation plots, that have been scaled by a factor of 7 in order to be superimposed on the feature projection graph. As already described, these arrows show the direction of the original features in the space of the two first principal components. We only kept the arrows with a magnitude greater than 0.7.

The mean, the standard deviation and the rank of the most significant features are displayed in **Table 2** for each one of the 5 clusters. These features are the 5 best for each cluster according to the rank test presented in Supplementary Material. It also shows some classical features used to predict CRT response. We can note that clinical features show a lower ranking compared to those obtained from strain integrals. The only clinical features with high ranking, in addition to those presented in **Table 2**, are the Ischemic etiology for cluster 1 and Gender for cluster 4. Global myocardial work and Constructive myocardial work were particularly interesting for cluster 2, respectively ranked 9 and 6.

According to these results, **Figure 3** summarizes the most significant features characterizing each cluster, presented in order of their importance. For each cluster, features with higher values compared to their value in other clusters are shown in a box named “High value”. The same was done for features showing medium and low values. For instance, patients in cluster 2 have a relatively high QRS, medium P^{Mean} and low I_{peak}^{Mean} with respect to the other clusters, so QRS are in “High value” box, P^{Mean} in “Medium value” and I_{peak}^{Mean} in “Low value” for cluster 2.

The most significant features characterizing patients in cluster 5 are the strain integrals, especially I_{avc}^{L} and I_{avc}^{D}. I_{avc}^{L} quantifies the cumulative strain developed by the lateral wall, which effectively contributes to LV ejection and I_{avc}^{D} represents the difference of the cumulative strain developed by each wall to eject blood.

In contrast to cluster 5, that is characterized by a high I_{avc}^{L} and I_{avc}^{D}, these strain integrals are low for cluster 1, showing the worst responder rate. The highly-ranked, SF and AR are low for the patients of cluster 1 and the ischemic etiology is high (explaining probably why other highly-ranked integral strains are also low in this cluster). We can also note low values of LBBB morphology. These characteristics are consistent with known data for poor responders [9] [10] [11].

Clusters 2 and 3 have similar response rates, but they differ by their features. Indeed, cluster 2 shows the lowest LVEF, GLS and constructive work. In contrast, cluster 3 shows the highest LVEF, GLS and constructive work. Some integrals are important for one or two of these clusters, mainly concerning the septal wall and the mean of integrals: I_{avc}^{MS}, I_{avc}^{Mean}, I_{avc}^{S}, I_{peak}^{Mean}, I_{peak}^{S}. Value of peak of strain are also important for these clusters: P^{Mean} and P^{MS}. Clusters 2 and 3 show an average response rate to CRT, so their corresponding features were considered as less useful to estimate response to CRT.

Cluster 4 has a better response to CRT (85.7%). The most significant features are different from the other clusters. Indeed, this is the only cluster where time to peak strain (T type) and integrals between the strain peak and the aortic valve closure (E type) are significant contributors. For clinical features, gender is only useful to separate cluster 4 from the others but constructive work is the only highly-ranked feature of cluster 4 which has a high rank for several other clusters too.

Strain traces analysis

The barycenter of each cluster was detected as the vector obtained by calculating the mean of each feature within a given cluster. The patient that was the closest to each barycenter was considered as a "representative" patient for the corresponding cluster and was selected for strain analysis. **Figure 4** displays the observed strain signals of these representative patients of each cluster.

Kaplan Meier analysis

Kaplan Meier curves for event free survival at 4 years are displayed in **Figure 5**. We observed a 22.8% overall adverse event rate (death and hospitalization for heart failure) in the whole population. The mean duration of follow up was 3.7 years. It is interesting to note the stark contrast between the low event rate in cluster 5 (7.3 %) and the very high event rate in cluster 1 (36.5%). The other groups are almost equal (respectively 13.8%, 13.8%, 14.3% in clusters 2, 3 and 4).

There was a significant difference in overall event-free survival at 4 years with $p<0.001$, and between clusters 1 and 2 ($p=0.004$), 1 and 3 ($p=0.033$), 1 and 4 ($p=0.004$), 1 and 5 ($p=0.003$). There is no significant difference between the others ($p>0.05$).

The adverse event rate is similar to the response for every cluster, except cluster 4. The features associated with a good response are the same for good survival (cluster 5). The

same conclusion can be made for the lack of response and low survival (cluster 1). Cluster 2 and 3 have similar survival as well as average response rate. Cluster 4 shows a similar adverse event rate than clusters 2 and 3, but with a higher response rate to CRT. The features that best separate this cluster from the others are thus interesting potential markers to detect response to CRT, but with lack of sensitivity on increased survival.

Discussion

Unsupervised machine learning allows for an integration of echocardiographic data (deformation parameters quantified automatically), as well as ECG and clinically meaningful data into a comprehensive analysis of CRT response. We identified 5 phenogroups with different profiles of CRT response. Our work exploits morphological features of strain curves that have shown to be of particular significance(5, 10).

Clustering

Traditionally, much of the research in cardiology comes from conventional hypothesis-driven studies that explore a small number of preselected features in limited datasets and their impact on treatment and prognosis, and statistical methods such as logistic or linear regression analysis. To define CRT response, we are limited to the initially proposed determinants without any convincing demonstration that imaging tools could help(1, 10, 19) . Machine learning-based methods can process a large number of variables in a hypothesis-free approach. It might help move from “evidence-based medicine” to data-driven precision medicine(20, 21). Clustering approaches have been developing recently because they could help better understand diseases, and define subgroups of similar patients in a heterogenous population(20, 22-24). Our current interpretation relies on a few parameters for patient selection and our strain quantification relies on a learning curve and expertise for a limited number of selected parameters, such as peaks or time to peaks, which might not capture the

information content throughout the cardiac cycle. The proposed feature extraction and machine learning methods go beyond clinical experience and the limited number of standard parameters, by capturing and integrating the complex and complete information from myocardial mechanics throughout the cardiac cycle. Unsupervised clustering allows for the integration of clinical data and for the representation of a given individual into an output space, within one of the defined clusters, whereby the likelihood to respond to CRT can be better predicted. The originality of our approach resides in the features we imputed in our clustering algorithm. We applied a quantitative approach to clustering, with analysis of strain integrals, as well as classical clinical and echocardiographic features. It complements our previous work, firstly by extending the number of features extracted from strain curves and secondly by providing a combined analysis with clinical features(5). The approach is different from the work by Cikes et al, which is based on the analysis of echocardiographic data of a large randomized study, where the strain curves were exploited only through qualitative markers(10). The obtained results from the clustering phase allows for the identification of groups of different response rates, ranging from below-average to above-average. In our work, which included patients who were implanted based on current CRT guidelines (1), cluster 1 had a response rate of 50.0 %. The negative predictive value of this approach is low. However, clustering produces subgroups of similar patients that can then be analyzed based on a multitude of characteristics. We applied factorial plans and rank tests to understand cluster differentiation. We can note that features which compose the first factorial plane are essentially obtained from strain integral analysis and this first factorial plane explains 33.6% of the variance of the whole feature space. It should be emphasized that all the available variables were used for rank test characterization between different clusters, providing a wide analysis for the identification of the most informative features differentiating any

cluster from the others. Traditional features (QRS-morphology or duration, LVEF, NYHA) do not help to define clusters in our selected population. The construction of the included patient population can be the cause. Indeed, every patient has broad QRS with LBBB morphology creating a population with homogeneous traditional features.

Adverse event rate, super response (cluster 5) to low probability of response (cluster1)

In our study, 74% of patients responded to CRT with ≥15% decrease in LVESV, which is comparable to response rate described in the literature(1, 25). We observed a 22.8% overall adverse event rate (death and hospitalization for heart failure), which is coherent with known data(25).

Patients in Cluster 5 show an outcome that can be compared to that of super responders, described previously in the literature(26, 27). Super response has different definitions, either LVEF≥50% or in the highest quartile or absolute change of LVEF ≥15% or LV end-systolic volume reduction of ≥30% at 6 months(7, 27). Average LVEF in cluster 5 at 6-months post CRT was 48.6%, with an improvement in LVEF of +18.2 %, making patients in this group super responders, whereas average LVEF post CRT was 35.7% in cluster 1 (+5.6%), 32.8% in cluster 2 (+11.2%), and 45.3% in cluster 3 (+12%). Cluster 4 also presented a good response profile with post CRT LVEF at 46.6% with +17.7% LVEF improvement.

Strain trace morphology of cluster 5 (**Figure 4-E**) shows a typical LBBB activation pattern with early stretching of lateral wall and early shortening of septal wall, early (<70% ejection time) peak septal contraction, and late lateral peak contraction, after aortic valve closure. This typical LBBB pattern is known to be associated with an improved prognosis after CRT [7]. Indeed, SF and AR, as well as typical LBBB strain trace pattern reflect specific electromechanical dyssynchrony, which is the target of CRT [8]. Nevertheless, the rank of these three features is rather low for cluster 5. This is certainly due to close results with

cluster 4. Indeed, both of them have high SF, AR and LBBB. SF and AR have already been shown to be associated with CRT response and better prognosis [6]. We can also note that the patients in clusters 4 and 5 show a low rate of ischemic etiology, low occurrence of MR, high wasted myocardial work and high constructive myocardial work. These results are consistent with our recent work on myocardial work indices [4 5].

In contrast, cluster 1 shows the worst responder rate and the worst adverse event rate. Strain trace morphology in cluster 1 (**Figure 4-A**) shows an atypical LBBB morphology, with some early stretching of the lateral wall, non-early peak septal shortening close to aortic valve closure, and peak lateral shortening during or shortly after aortic valve closure. Patients in cluster 1 therefore do not present true electromechanical dyssynchrony, but rather a non-electrical scar substrate of mechanical dyssynchrony, on which CRT is less effective by two mechanisms: presence of scar tissue on the area of LV lead placement and reduced myocardial viability [8 14]. Precise mapping of the scar areas by multimodality imaging would be particularly interesting in this group to improve LV lead placement, which has been shown to improve CRT response [15].

It is also interesting to note that the group with the worst prognosis is cluster 1, the worst responder, but patients in cluster 2, the group with the most severe cardiomyopathy, lowest LVEF, GLS and remodeled LV, have a response rate of 70.8%, and a significantly better prognosis than cluster 1, with an adverse event rate of 13.8% at 4 years versus 36.5% (p=0.004). This means that even patients with advanced cardiomyopathy and severe remodeling can benefit from CRT, but those who do not respond to CRT have a very poor prognosis and must be identified early, to adapt therapy and follow up. Machine learning approaches can help identify these patient profiles.

Demonstration of the real value of strain curves for analyzing mechanical dyssynchrony

The role of longitudinal strain integrals in understanding left ventricular mechanics has already been highlighted [16], and our study shows the added value of using strain integrals in a clustering approach to improve phenogroup differentiation with better granularity. Indeed, integrals of strain, such as I_{avc}^{L}, I_{avc}^{D}, I_{peak}^{L} and I_{peak}^{D}, can differentiate super responders (high value), usual responders (medium value) and bad responders (low values). However, septal wall strain integrals do not discriminate well between good and bad responders, except for cluster 4 with integrals such as E^{S}.

I_{avc}^{L} represents a quantification of the cumulative strain developed by all the lateral segments, which effectively contributes to LV ejection. This could be a marker of residual lateral wall contraction. Stimulation of the lateral wall is a target of CRT therapy, and the amount of mechanical energy which can be developed by this wall is known to be associated to CRT response [15].

I_{peak}^{L} corresponds to the global cumulative strain developed by the contraction of the lateral wall and is an indirect marker of lateral wall viability. In patients undergoing CRT, the delayed activation of the lateral wall occurs after aortic valve closure, meaning only a part of the cumulative strain developed by the lateral wall contributes to LV ejection.

Strain integrals also differentiate clusters of similar patients. Indeed, in clusters 4 and 5, which present similar profiles of CRT response (respectively 85.7% and 92.7%) but different post CRT outcomes with a 2-fold risk of death or hospitalization for heart failure in cluster 4 (14.3% versus 7.3% in cluster 5), classical clinical and echocardiography parameters fall short to differentiate these clusters and some strain trace characteristics are similar with SF and AR. However, strain integral features differ, with high integrals of strain (I_{avc} and I_{peak} types) in cluster 5 and low integrals of strain (E types) in cluster 4 as represented in **Figure 3**.

Limitations

The quality of data relies on acquired images and their quality, which is an inherent limit in all echocardiographic studies, but we minimized this limitation by excluding echo exams with unacceptable 2D image quality. Future studies with more subjects and automated measurements could allow for a more detailed clustering and patient-specific approach, where machine-learning could be implemented to predict response and prognosis for each patient. Patients in atrial fibrillation were not considered in this study. Validation of the present results on another cohort has not been yet performed. We focused the analysis on the description of the clusters and the value of the concept.

As we can see in **Figure 2**, our data contains outliers. Clustering such as K-means can be sensitive to such data.

Some error can appear in the classification with the rank test analysis due to many statistical tests performed.

We acknowledge that the success of CRT is dependent upon proper location of the LV pacing lead. The LV lead was positioned at the discretion of the implanter though the goal was to achieve the shortest QRS duration.

Conclusions

Clustering applied to CRT recipients allows for the identification of specific subgroups of CRT response and outcome. This provides information about indicators of low response, as well as very good response. Automatic quantitative longitudinal strain curve analysis offers a good discriminative value between clusters, more than classical clinical and echocardiographic features, and appears as a promising tool to improve the understanding of LV mechanics and to improve patient characterization and selection for CRT.

References

1. Ponikowski P, Voors AA, Anker SD, Bueno H, Cleland JGF, Coats AJS, et al. 2016 ESC Guidelines for the diagnosis and treatment of acute and chronic heart failure: The Task Force for the diagnosis and treatment of acute and chronic heart failure of the European Society of Cardiology (ESC)Developed with the special contribution of the Heart Failure Association (HFA) of the ESC. Eur Heart J. 2016;37(27):2129-200.
2. Yancy CW, Jessup M, Bozkurt B, Butler J, Casey DE, Jr., Colvin MM, et al. 2017 ACC/AHA/HFSA Focused Update of the 2013 ACCF/AHA Guideline for the Management of Heart Failure: A Report of the American College of Cardiology/American Heart Association Task Force on Clinical Practice Guidelines and the Heart Failure Society of America. J Am Coll Cardiol. 2017;70(6):776-803.
3. Galli E, Leclercq C, Donal E. Mechanical dyssynchrony in heart failure: Still a valid concept for optimizing treatment? Arch Cardiovasc Dis. 2017;110(1):60-8.
4. Donal E, Delgado V, Magne J, Bucciarelli-Ducci C, Leclercq C, Cosyns B, et al. Rational and design of EuroCRT: an international observational study on multi-modality imaging and cardiac resynchronization therapy. Eur Heart J Cardiovasc Imaging. 2017;18(10):1120-7.
5. Bernard A, Donal E, Leclercq C, Schnell F, Fournet M, Reynaud A, et al. Impact of Cardiac Resynchronization Therapy on Left Ventricular Mechanics: Understanding the Response through a New Quantitative Approach Based on Longitudinal Strain Integrals. J Am Soc Echocardiogr. 2015;28(6):700-8.
6. Galli E, Leclercq C, Hubert A, Bernard A, Smiseth OA, Mabo P, et al. Role of myocardial constructive work in the identification of responders to CRT. Eur Heart J Cardiovasc Imaging. 2018;19(9):1010-8.
7. Vaillant C, Martins RP, Donal E, Leclercq C, Thebault C, Behar N, et al. Resolution of left bundle branch block-induced cardiomyopathy by cardiac resynchronization therapy. J Am Coll Cardiol. 2013;61(10):1089-95.
8. Lumens J, Leenders GE, Cramer MJ, De Boeck BW, Doevendans PA, Prinzen FW, et al. Mechanistic evaluation of echocardiographic dyssynchrony indices: patient data combined with multiscale computer simulations. Circ Cardiovasc Imaging. 2012;5(4):491-9.
9. Risum N, Tayal B, Hansen TF, Bruun NE, Jensen MT, Lauridsen TK, et al. Identification of Typical Left Bundle Branch Block Contraction by Strain Echocardiography Is Additive to Electrocardiography in Prediction of Long-Term Outcome After Cardiac Resynchronization Therapy. J Am Coll Cardiol. 2015;66(6):631-41.
10. Cikes M, Sanchez-Martinez S, Claggett B, Duchateau N, Piella G, Butakoff C, et al. Machine learning-based phenogrouping in heart failure to identify responders to cardiac resynchronization therapy. Eur J Heart Fail. 2019;21(1):74-85.
11. Stankovic I, Prinz C, Ciarka A, Daraban AM, Kotrc M, Aarones M, et al. Relationship of visually assessed apical rocking and septal flash to response and long-term survival following cardiac resynchronization therapy (PREDICT-CRT). Eur Heart J Cardiovasc Imaging. 2016;17(3):262-9.
12. Hasselberg NE, Haugaa KH, Bernard A, Ribe MP, Kongsgaard E, Donal E, et al. Left ventricular markers of mortality and ventricular arrhythmias in heart failure patients with cardiac resynchronization therapy. Eur Heart J Cardiovasc Imaging. 2016;17(3):343-50.
13. Hubert A, Le Rolle V, Leclercq C, Galli E, Samset E, Casset C, et al. Estimation of myocardial work from pressure-strain loops analysis: an experimental evaluation. Eur Heart J Cardiovasc Imaging. 2018;19(12):1372-9.
14. Russell K, Eriksen M, Aaberge L, Wilhelmsen N, Skulstad H, Remme EW, et al. A novel clinical method for quantification of regional left ventricular pressure-strain loop area: a non-invasive index of myocardial work. Eur Heart J. 2012;33(6):724-33.
15. Galli E, Leclercq C, Fournet M, Hubert A, Bernard A, Smiseth OA, et al. Value of Myocardial Work Estimation in the Prediction of Response to Cardiac Resynchronization Therapy. J Am Soc Echocardiogr. 2018;31(2):220-30.

16. . !!! INVALID CITATION !!! 5.
17. Etchepareborda P, Federico A, Kaufmann GH. Sensitivity evaluation of dynamic speckle activity measurements using clustering methods. Appl Opt. 2010;49(19):3753-61.
18. Ioannou A, Fokianos K, Promponas VJ. Spectral density ratio based clustering methods for the binary segmentation of protein sequences: a comparative study. Biosystems. 2010;100(2):132-43.
19. Lecoq G, Leclercq C, Leray E, Crocq C, Alonso C, de Place C, et al. Clinical and electrocardiographic predictors of a positive response to cardiac resynchronization therapy in advanced heart failure. Eur Heart J. 2005;26(11):1094-100.
20. Shameer K, Johnson KW, Glicksberg BS, Dudley JT, Sengupta PP. The whole is greater than the sum of its parts: combining classical statistical and machine intelligence methods in medicine. Heart. 2018;104(14):1228.
21. Shameer K, Johnson KW, Glicksberg BS, Dudley JT, Sengupta PP. Machine learning in cardiovascular medicine: are we there yet? Heart. 2018;104(14):1156-64.
22. Omar AMS, Narula S, Abdel Rahman MA, Pedrizzetti G, Raslan H, Rifaie O, et al. Precision Phenotyping in Heart Failure and Pattern Clustering of Ultrasound Data for the Assessment of Diastolic Dysfunction. JACC Cardiovasc Imaging. 2017;10(11):1291-303.
23. Lancaster MC, Salem Omar AM, Narula S, Kulkarni H, Narula J, Sengupta PP. Phenotypic Clustering of Left Ventricular Diastolic Function Parameters: Patterns and Prognostic Relevance. JACC Cardiovasc Imaging. 2019;12(7 Pt 1):1149-61.
24. Dey D, Slomka PJ, Leeson P, Comaniciu D, Shrestha S, Sengupta PP, et al. Artificial Intelligence in Cardiovascular Imaging: JACC State-of-the-Art Review. J Am Coll Cardiol. 2019;73(11):1317-35.
25. Daubert C, Behar N, Martins RP, Mabo P, Leclercq C. Avoiding non-responders to cardiac resynchronization therapy: a practical guide. Eur Heart J. 2017;38(19):1463-72.
26. Hsu JC, Solomon SD, Bourgoun M, McNitt S, Goldenberg I, Klein H, et al. Predictors of super-response to cardiac resynchronization therapy and associated improvement in clinical outcome: the MADIT-CRT (multicenter automatic defibrillator implantation trial with cardiac resynchronization therapy) study. J Am Coll Cardiol. 2012;59(25):2366-73.
27. van der Heijden AC, Hoke U, Thijssen J, Willem Borleffs CJ, Wolterbeek R, Schalij MJ, et al. Long-Term Echocardiographic Outcome in Super-Responders to Cardiac Resynchronization Therapy and the Association With Mortality and Defibrillator Therapy. Am J Cardiol. 2016;118(8):1217-24.

Figures:

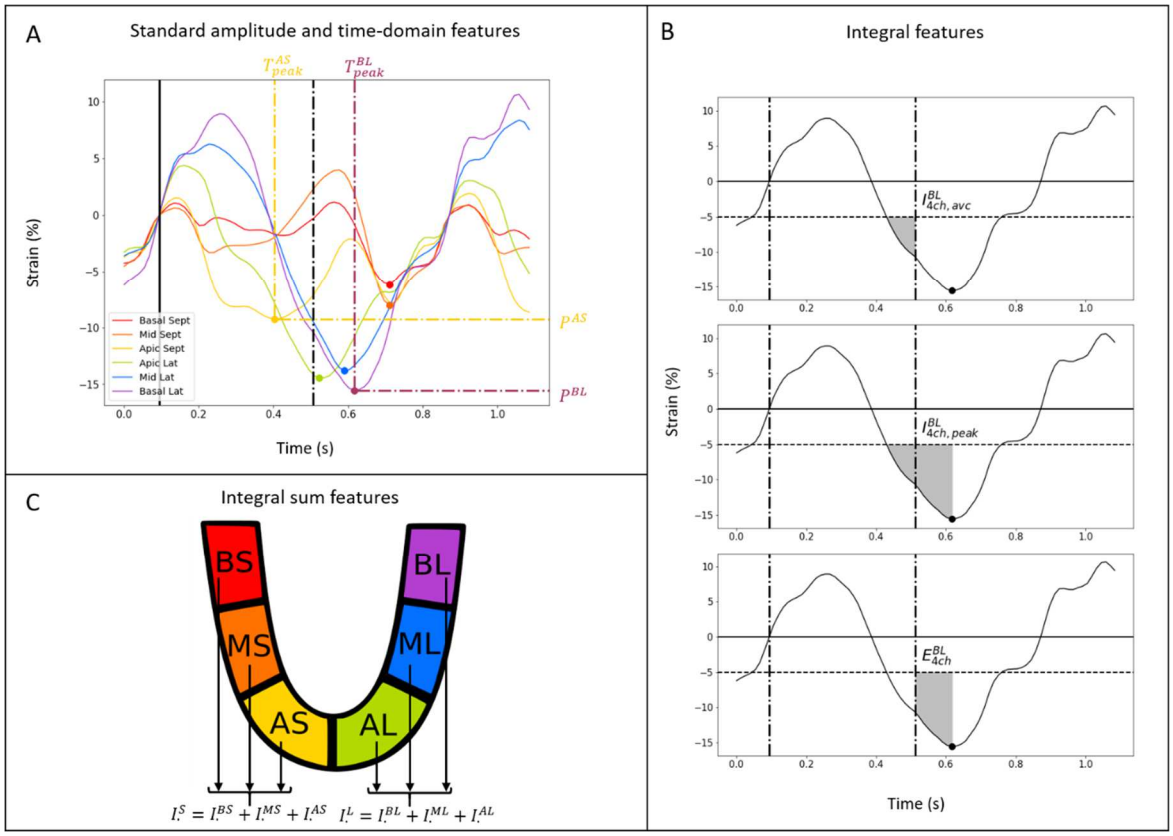

Figure 1. Feature extraction from longitudinal strain time series. A) Longitudinal strain signals for all segments showing standard amplitude and time-domain features extracted automatically from these signals. The black solid line corresponds to the onset of the QRS and the black dotted line is the aortic valve closure. The colored dots correspond to the peak of stain for each one of the six segments. B) Example calculation of the three kinds of strain integrals (grey zones) from the longitudinal strain signal of segment BL. The upper panel shows the integral value calculated before the aortic valve closure (I_{avc}^{BL}). The middle panel depicts the integral calculated up to the strain peak (I_{peak}^{BL}). The lower panel shows the difference between the two preceding integral calculations (E^{BL}). Note that all integrals are calculated for values lower than 5%. C) Identification of the different segments, showing how the sum of integrals for different segments are calculated (B: basal, M: Mid, and A: Apical, S: Septal and L: Lateral).

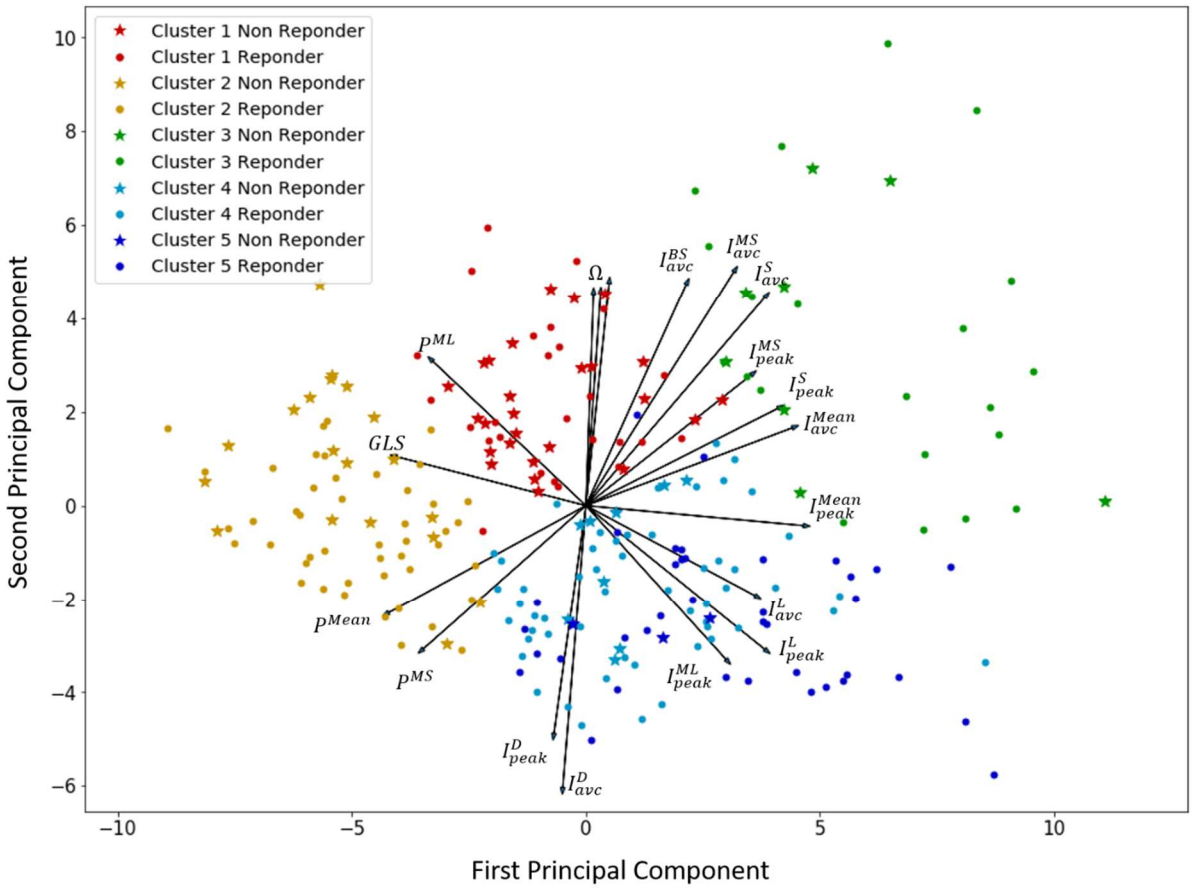

Figure 2. Results obtained from the application of a principal component analysis (PCA) to the available data. Only the first plane, composed of the first two principal components is displayed, allowing for a 2D representation of the underlying 70-dimensions space. In this plane, each dot represents a patient and each color represents a different cluster. Responders are marked with a star. The black arrows represent a variable correlation plot. The direction of each arrow represents the direction in which a given variable (noted at the tip of each arrow) contributes to the representation of the data in the plane. Ω represents, from left to right, E^{BS}, E^{MS} and E^{S}. *GLS: global longitudinal strain,* P^{ML} *and* P^{MS}*: amplitude of the peak of strain for ML and MS,* P^{Mean}*: average of all amplitude of peak of strain,* I^{BS}_{avc} *and* I^{MS}_{avc}*: integral between QRS onset and aortic valve closure for BS and MS,* I^{Mean}_{avc}*: mean of all integral between QRS onset and aortic valve closure,* I^{S}_{avc} *and* I^{L}_{avc}*: sum of the integral between QRS onset and aortic valve closure for each wall,* I^{D}_{avc}*: difference between* I^{S}_{avc} *and*

I^{L}_{avc}, I^{MS}_{peak} and I^{ML}_{peak}: integral between QRS onset and peak of strain for MS and ML, I^{Mean}_{peak}: mean of all integral between QRS onset and peak of strain, I^{S}_{peak} and I^{L}_{peak}: sum of the integral between QRS onset and peak of strain for each wall, I^{D}_{peak}: difference between I^{S}_{peak} and I^{L}_{peak}, E^{BS} and E^{MS}: integral between aortic valve closure and peak of strain for BS and MS, E^{S}: sum of the integral between aortic valve closure and peak of strain for septal wall.

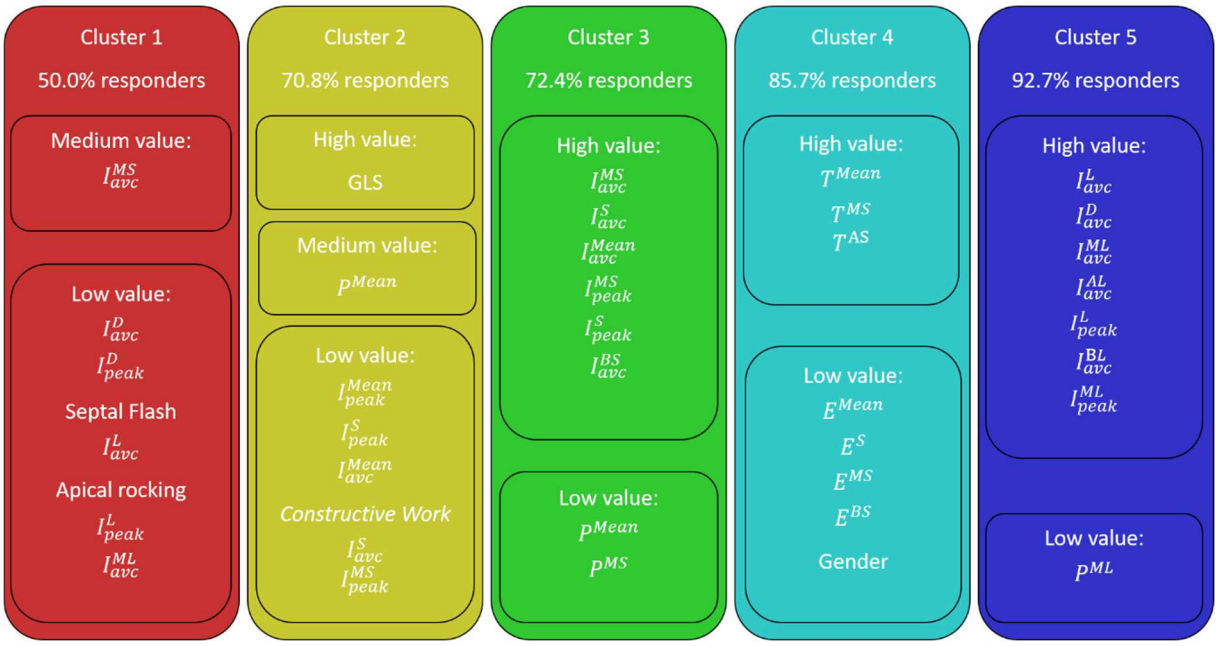

Figure 3. Most significant features with high, medium or low values for each cluster, listed by level of importance. *GLS: global longitudinal strain*

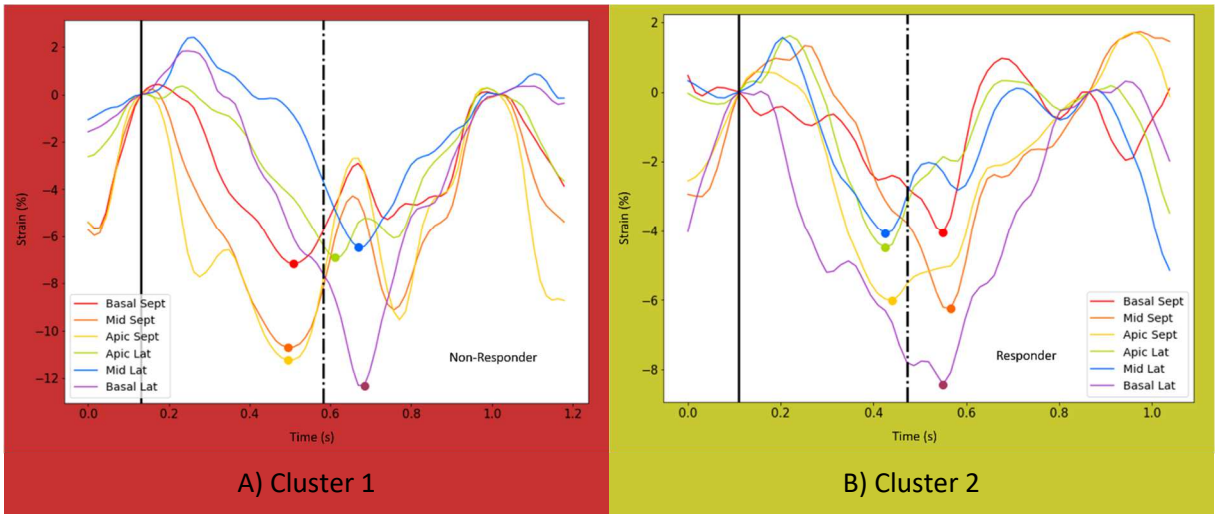

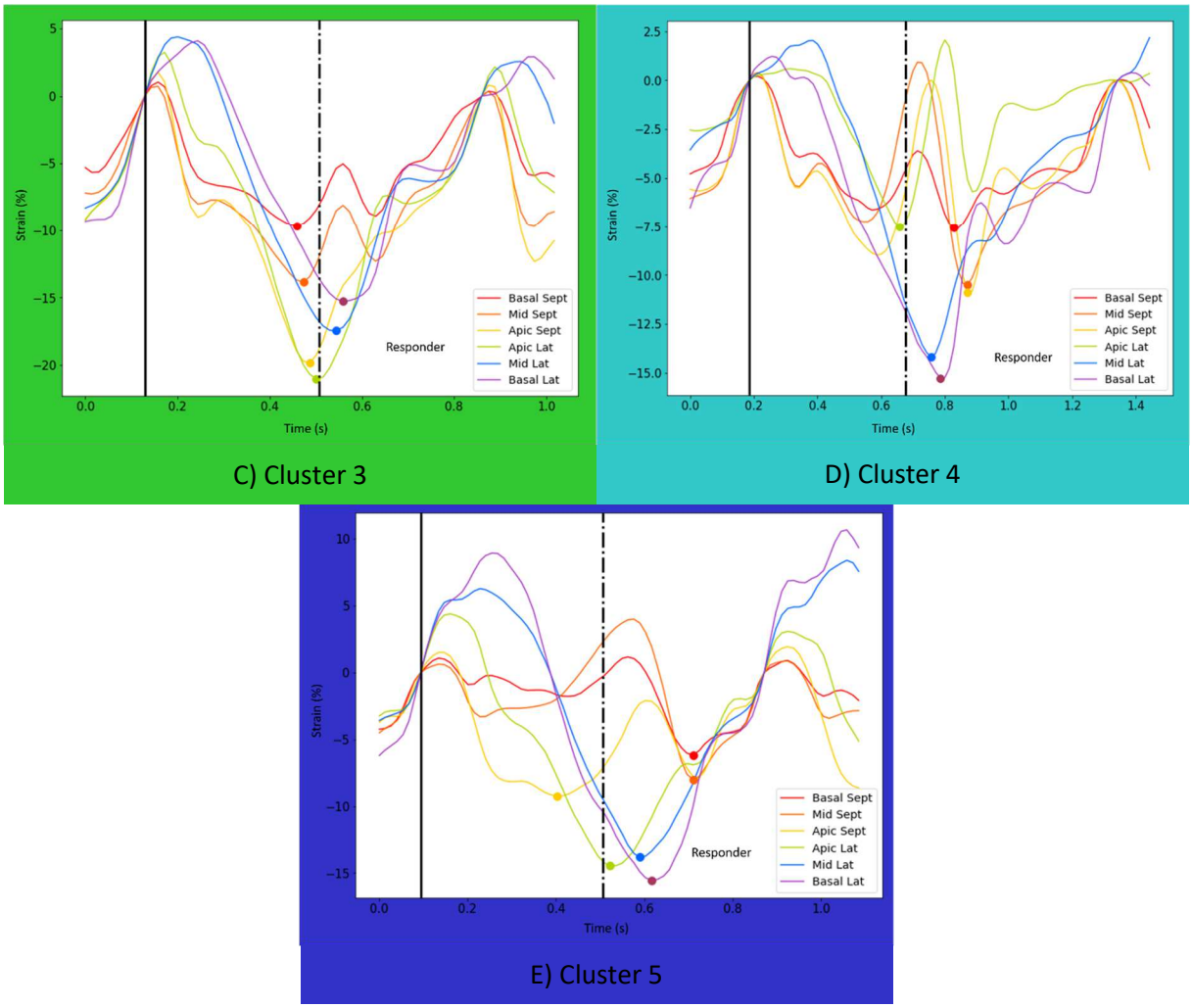

Figure 4. Strain curves representative patients of each cluster (the closest to the barycenter). The black solid line corresponds to the onset of the QRS and the black dotted line is the aortic valve closure. The black dots correspond to the value of strain for the six segments at the aortic valve closure. The colored dots correspond to the peak of stain for the six segments. A) Strain curves of the patient of cluster 1 (dyssynchrony but severely impaired myocardial longitudinal deformation). B) Strain curves of the patient of cluster 2 (less dyssynchrony at the apex, impaired myocardial longitudinal deformation). C) Strain curves of the patient of cluster 3 (early deformation of the septum resulting in stretching of the lateral wall with an overall reduced alteration of regional myocardial deformation). D) Strain curves of the patient of cluster 4 (close to cluster 4, but with much more pronounced

dyscoordination between septal and lateral walls). E) Strain curves of the patient of cluster 5 (the most discordant deformation between septal and lateral LV-walls).

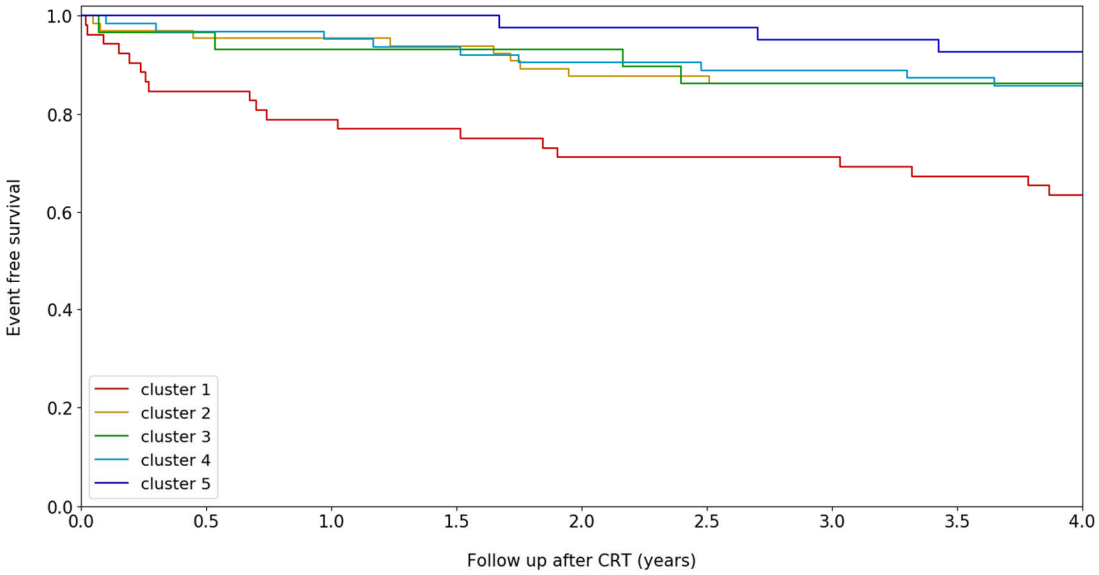

Cluster 1	52	44	41	40	37	37	37	35	33
Cluster 2	65	62	62	61	57	57	56	56	56
Cluster 3	29	28	27	27	27	25	25	25	25
Cluster 4	63	61	60	59	57	56	56	55	54
Cluster 5	41	41	41	41	40	40	39	38	38

Figure 5. Kaplan Meier survival curve at 4 years with the numbers at risk.

Tables

Table 1. Patient characteristics of the whole studied population and for responders and non-responders. Results are presented as mean±sd, except for binary features such as Gender or Hypertension which are presented as percentage. Features with a * marker have a significant P-value (<0.05) between Responders and Non-Responders.

	Overall population	Responders	Non-Responders	P-value
Number of patients (%)	250 (100%)	185 (74%)	65 (26%)	
Gender, % of males *	65.6	60.0	81.5	0.002
Age (years)	67.2 ± 10.9	67.2 ± 10.9	67.1 ± 10.8	0.96
Ischemic etiology, % *	31.2	23.2	53.8	<0.001
Moderate to severe MR, %	9.6	9.7	9.2	0.91
Diabetes mellitus, %	18.4	15.67568	26.15385	0.068
Hypertension, %	30.8	30.27027	32.30769	0.76
NYHA functional class	2.3 ± 0.7	2.3 ± 0.6	2.4 ± 0.8	0.26
Creatinine (µmol)	92.2 ± 36.1	92.5 ± 33.5	91.5 ± 42.7	0.85
QRS duration (ms) *	161.7 ± 23.0	163.7 ± 20.7	155.7 ± 27.7	0.015
LBBB, % *	87.2	91.4	75.4	<0.001
Left atrial volume (mL/m^2) *	45.1 ± 16.1	43.8 ± 16.4	48.6 ± 14.9	0.042
LVEDV (mL)	216.2 ± 73.8	211.3 ± 75.6	230.1 ± 66.6	0.077
LVESV (mL)	156.8 ± 62.8	154.2 ± 63.7	164.2 ± 59.5	0.27
LVEF (%)	28.0 ± 6.6	27.9 ± 6.3	28.5 ± 7.3	0.51
SF, % *	68.4	82.70	27.69	<0.001
AR, % *	65.2	74.59	38.46	<0.001
E/e' ratio *	13.9 ± 7.9	12.8 ± 7.7	17.1 ± 7.8	<0.001
TAPSE *	19.0 ± 5.1	19.6 ± 4.8	17.2 ± 5.5	<0.001
Right ventricular strain (%) *	-15.5 ± 10.1	-16.3 ± 10.0	-13.1 ± 10.2	0.027
SPAP (mm Hg)	21.6 ± 20.6	21.7 ± 19.9	21.3 ± 22.6	0.90
GLS (%) *	-8.6 ± 3.3	-9.0 ± 3.3	-7.3 ± 2.7	<0.001
Dispersion (strain peaks) (ms)	93.6 ± 49.0	96.6 ± 46.0	85.1 ± 55.7	0.10

LBBB: left bundle branch block morphology, LVEDV: left ventricular end-diastolic volume, LVESV: left ventricular end-systolic volume, LVEF: left ventricular ejection fraction, SF: septal flash, AR: apical rocking, TAPSE: tricuspid annular plan systolic excursion, GLS: global longitudinal strain.

Table 2. Main features for each one of the 5 identified clusters and some clinical features. Results are presented as mean±sd (rank), except SF, AR, LBBB and Ischemic etiology which are presented as percentage (rank).

	Cluster 1	Cluster 2	Cluster 3	Cluster 4	Cluster 5
I_{avc}^{D}	-2.86 ± 2.05 (1)	0.77 ± 1.90 (43)	-4.18 ± 3.27 (11)	0.14 ± 2.34 (63)	4.34 ± 2.31 (2)
I_{peak}^{D}	-1.36 ± 2.58 (2)	1.37 ± 1.51 (42)	-1.89 ± 3.04 (27)	0.49 ± 2.68 (67)	3.22 ± 2.39 (11)
SF, %	38.5 (3)	60.0 (51)	65.5 (67)	92.1 (15)	85.4 (32)
I_{avc}^{L}	2.26 ± 1.64 (4)	1.98 ± 1.58 (22)	6.86 ± 2.77 (15)	3.70 ± 1.65 (70)	8.67 ± 2.14 (1)
AR, %	36.5 (5)	64.6 (69)	34.5 (30)	88.9 (18)	87.8 (25)
I_{peak}^{Mean}	1.25 ± 0.36 (50)	0.58 ± 0.31 (1)	2.50 ± 0.70 (9)	1.66 ± 0.54 (22)	1.93 ± 0.64 (17)
I_{peak}^{S}	4.42 ± 1.68 (41)	1.05 ± 0.89 (2)	8.46 ± 2.78 (7)	4.74 ± 2.34 (30)	4.17 ± 2.34 (56)
GLS	-8.1 ± 2.1 (51)	-5.1 ± 1.7 (3)	-11.7 ± 3.1 (18)	-9.9 ± 2.6 (17)	-10.5 ± 2.2 (19)
P^{Mean}	-9.34 ± 2.01 (37)	-4.01 ± 2.42 (4)	-14.01 ± 2.06 (3)	9.18 ± 2.44 (41)	8.79 ± 2.62 (57)
I_{avc}^{Mean}	1.23 ± 0.42 (63)	0.53 ± 0.33 (5)	2.98 ± 0.73 (4)	1.21 ± 0.51 (60)	2.16 ± 0.58 (10)
I_{avc}^{MS}	1.81 ± 0.93 (8)	0.26 ± 0.46 (14)	4.00 ± 1.02 (1)	1.03 ± 0.87 (57)	0.94 ± 0.80 (53)
I_{avc}^{S}	5.12 ± 1.59 (13)	1.21 ± 1.13 (7)	11.04 ± 2.68 (2)	3.56 ± 2.17 (58)	4.29 ± 2.03 (50)
P^{MS}	-9.91 ± 2.75 (20)	-3.54 ± 3.63 (10)	-14.03 ± 2.15 (5)	-8.79 ± 3.13 (54)	-7.76 ± 3.26 (52)
E^{Mean}	-0.02 ± 0.33 (56)	-0.05 ± 0.26 (55)	0.48 ± 0.81 (35)	-0.45 ± 0.40 (1)	0.23 ± 0.45 (22)
E^{S}	0.70 ± 1.38 (21)	0.16 ± 0.82 (66)	2.58 ± 3.07 (17)	-1.18 ± 1.39 (2)	0.12 ± 1.42 (64)
T^{Mean}	0.39 ± 0.12 (54)	0.23 ± 0.18 (12)	0.46 ± 0.10 (49)	0.53 ± 0.14 (3)	0.47 ± 0.18 (31)
E^{MS}	0.35 ± 0.77 (24)	0.05 ± 0.28 (57)	1.00 ± 1.36 (20)	-0.36 ± 0.59 (4)	-0.14 ± 0.45 (38)
E^{BS}	0.28 ± 0.58 (23)	0.10 ± 0.34 (54)	0.90 ± 0.99 (16)	-0.34 ± 0.57 (5)	-0.16 ± 0.43 (30)
I_{avc}^{ML}	0.51 ± 0.65 (7)	0.52 ± 0.69 (32)	1.78 ± 1.18 (33)	1.09 ± 0.90 (69)	2.82 ± 0.94 (3)

I_{avc}^{AL}	0.62 ± 0.79 (11)	0.47 ± 0.81 (28)	2.38 ± 1.66 (24)	1.25 ± 0.91 (56)	2.74 ± 1.28 (4)
I_{peak}^{L}	3.06 ± 1.68 (6)	2.42 ± 1.45 (16)	6.57 ± 2.39 (25)	5.23 ± 1.83 (28)	7.40 ± 2.18 (5)
QRS duration (ms)	156 ± 28 (48)	167 ± 24 (49)	160 ± 17 (51)	165 ± 14 (53)	157 ± 28 (60)
LVEF (%)	30.1 ± 4.5 (31)	21.6 ± 5.5 (11)	33.3 ± 5.1 (23)	29.0 ± 5.6 (61)	30.4 ± 5.4 (29)
LBBB, %	71.2 (15)	90.8 (59)	82.8 (60)	95.2 (38)	92.7 (51)
Ischemic etiology, %	55.8 (9)	30.8 (70)	41.4 (52)	17.5 (34)	14.6 (33)
Constructive work	929 ± 271 (38)	596 ± 256 (6)	1386 ± 395 (21)	1225 ± 372 (12)	1278 ± 347 (20)
Response rate, %	**50.0**	**70.8**	**72.4**	**85.7**	**92.7**

SF: Septal Flash, AR: Apical Rocking, GLS: global longitudinal strain, LVEF: left ventricular ejection fraction, LBBB: left bundle branch block morphology

Graphical abstract:

The physician get optimal images and optimal speckle tracking data

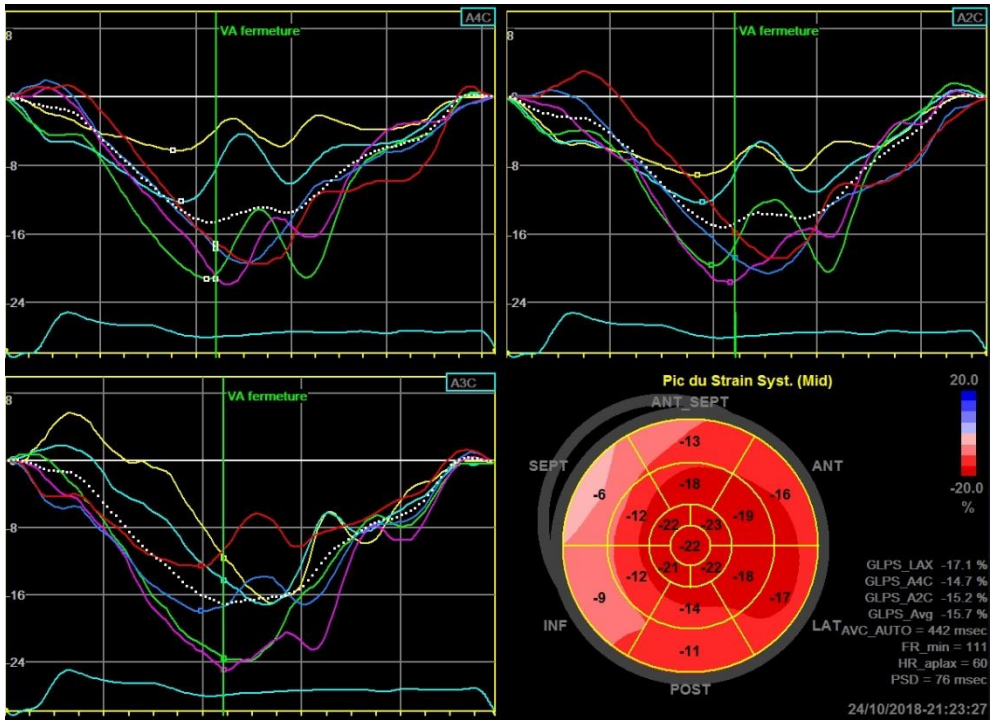

Automated extraction of strain feature that can be computed to provide clusters of patients

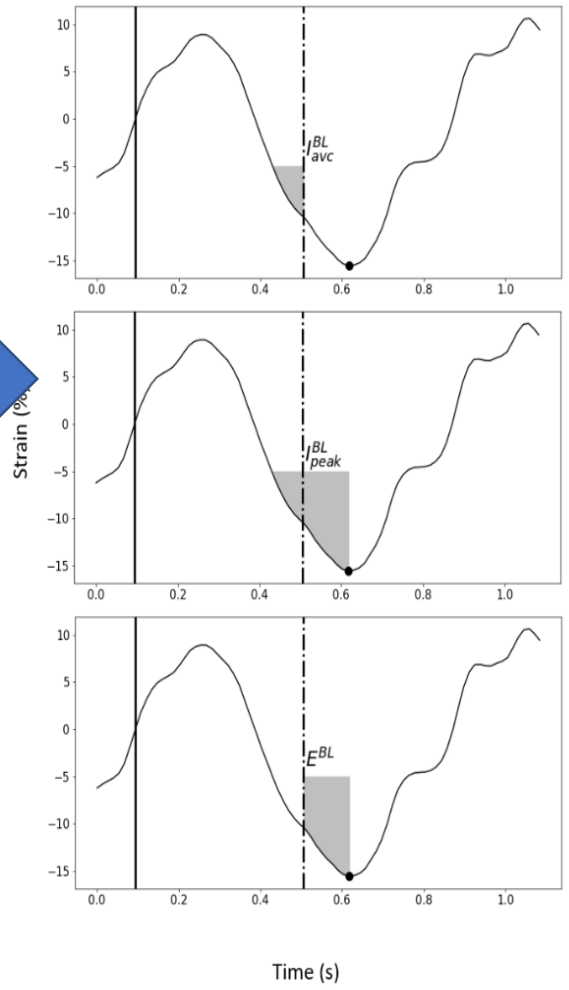

with distinct response to CRT and different prognosis